Microstructure and Mechanical Properties of Crack-Free IN738G Alloy Processed by Laser Powder Bed Fusion

Yi Wang[1], *Yue* Liu[1*], and *Quanquan* Han[1]

[1]Key Laboratory of High Efficiency and Clean Mechanical Manufacture of Ministry of Education, School of Mechanical Engineering, Shandong University, Jinan, 250061, China

Abstract. The IN738 nickel-based superalloy has a high Al, Ti and γ’ (Ni3 [Al, Ti]) content phase that causes notable crack sensitivity when processed by laser powder bed fusion (LPBF). After examining the effects of Ti and Co on the microstructure and mechanical properties of IN738 alloy processed by LPBF, this research revealed that a moderate decrease in Ti content and an increase in Co content resulted in a wide range of processing parameters to obtain crack-free LPBF specimens. The samples were treated by different heat-treatment processes and then investigated by scanning electron microscopy (SEM). The newly designed IN738G exhibited an excellent combination of tensile strength (1253.5 MPa) and elongation (16.37%) compared to the IN738 alloy (1115.7 MPa, 6.99%) under room-temperature conditions.

1 Introduction

IN738 is a nickel-based precipitation-strengthened casting superalloy that is mainly composed of Ni, Cr, Mo and other elements. Generally, it can maintain excellent mechanical properties and corrosion resistance in high-temperature environments below 900°C [1]. Laser powder bed fusion (LPBF), a laser additive manufacturing technology, has broad application prospects in the aerospace, automobile and gas-turbine production fields [2, 3], among others. Processing-related defects, especially cracks, remain challenging for the LPBF of traditional nickel-based superalloy materials [4], however.

When LPBF is used to process nickel-based superalloys with high cracking sensitivity, various defects (primarily solidification cracks, solid cracks and liquefaction cracks) [5] form due to such materials’ wide solidification temperature range, low melting point precipitation phase and relatively high residual stress. At present, some of the methods for crack suppression include (1) alloy element regulation, (2) printing process parameter optimisation and (3) the addition of heterogeneous nucleating agents [6]. Some scholars [7] have added 0.3–0.6 wt.% C element to IN738, successfully inhibiting solidification cracks. Some scholars [8] have reported that the mass fractions of Al and Ti are greater than 5 wt.% alloy and note that welding nickel-based superalloy can be difficult. The present study examines the formability and mechanical properties of IN738 alloy formed by LPBF. In this paper, the

* Corresponding author: liuyue@sdu.edu.cn

comparison is made between the content of Ti and Co, and changes in the microstructure are observed. The influence of Ti and Co on crack inhibition is discussed, leading to the proposal of an IN738G alloy with exceptional comprehensive mechanical properties suitable for LPBF forming.

2 Materials and methods

2.1 Materials

The particle size of the spherical gas-atomised IN738, LTi738 (1.5wt%Ti) and IN738G (1.08wt%Ti, 15.66wt%Co) powders used in this work was 15–53 µm. The chemical compositions of the three powders are shown in Table 1.

Table 1. IN738, LTi738 and IN738G powder compositions (wt%).

	Cr	Co	W	Mo	Al	Ti	Ta	Nb	C	Ni
IN738	15.92	8.12	3.75	1.66	3.20	3.34	1.64	0.83	0.17	Bal.
LTi738	15.92	8.12	3.75	1.66	3.20	1.50	1.64	0.83	0.17	Bal.
IN738G	17.63	15.66	3.75	1.66	3.20	1.08	1.64	0.83	0.09	Bal.

2.2 LPBF process

The LPBF process was carried out under argon protection using a Concept Laser Mlab custom 200R. For printing, a strip scanning strategy was adopted with 90° rotation for each scanning layer without preheating. The laser power, scan spacing and slice thickness of all samples were maintained at 190W, 0.04 mm and 0.11 mm, respectively; the scanning speed varied from 400 mm/s to 1400 mm/s to optimise the scanning speed value, which was found to be 900 mm/s.

2.3 Tensile testing

All tensile specimens were meticulously machined from a 75-mm-long slab that was initially fabricated through the LPBF process, as depicted in Fig. 1. The room-temperature tensile characteristics of the alloy, specifically its ultimate tensile strength (UTS) and total elongation (EL), were examined under a constant strain rate of 0.001 S^{-1}.

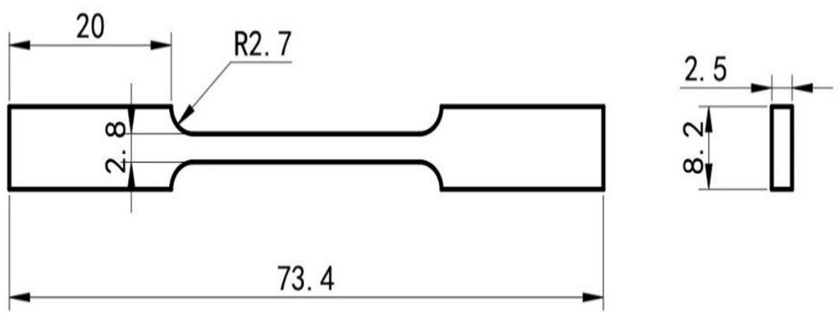

Fig. 1. Tensile specimen dimensions.

3 Results and discussion

3.1 Characterisation of defects and microstructure

The polished samples were placed under an optical microscope (OM) for observation; the results are shown in Fig. 2. At low scanning speeds, many keyholes were observed due to excessive energy density. When the scanning speed was increased to 1400 mm/s, the samples showed a lack of fusion defects, which was due to the low energy density. Cracks were observed in all IN738 samples, regardless of scanning speed. The LTi738 and IN738G alloys were found to be free from defects at scanning speeds of 600–1300 mm/s, which allowed crack-free printing of large process windows. A laser scanning speed of 900 mm/s was thus used to manufacture the tensile specimens.

In general, when the content of Ti is reduced, the risk of solid-state cracking is also reduced because of the decrease of the γ' phase content [9]. In this study, three materials were calculated by using JMatPro software. The results showed that the mass fraction of the γ' phase in IN738 alloy was 44.8% and 28.1% in LTi738 alloy, which was significantly lower. Interestingly, the mass fraction of the γ' phase in IN738G was found to be 31%.

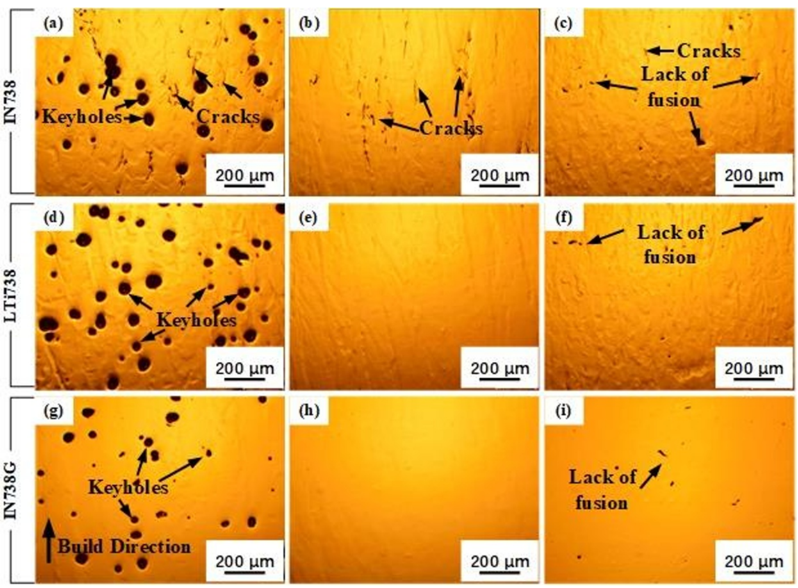

Fig. 2. Metallographic images of defect types and distribution of IN738, LTi738 and IN738G alloy samples prepared at different laser scanning speeds: (a), (d) and (g): 400 mm/s; (b), (e) and (h): 900 mm/s; (c), (f) and (i): 1400 mm/s.

Because Co is a solid solution strengthening element in nickel-based superalloys, it can reduce the solubility of Al and Ti in the matrix and improve the content of the γ' phase in the alloy. In this study, under the premise of further reducing the Ti element in IN738G alloy, increasing the Co element content not only significantly reduced the defect rate of samples but also improved the γ' phase content, which in general is beneficial for improving the high-temperature strength of the alloy.

3.2 Characterisation of heat-treated IN738G

In this study, we investigated the impact of heat treatment (HT) on IN738G alloy's microstructure and mechanical properties. We employed a three-stage HT strategy consisting of stress relief (SR) annealing, solution treatment and aging. The process entailed 24-hour stress relief annealing at 600°C, followed by a 2-hour solution treatment at 1120°C for all samples. Subsequently, a 24-hour aging treatment was conducted at 850°C, with specimens air-cooled (AC) to room temperature after each heat-treatment stage.

The etched specimens were observed using scanning electron microscopy (SEM); the results are shown in Fig. 3. The grains exhibited columnar structures, and we observed precipitates lining the grain boundaries. As depicted in Figure 3(b), we noted numerous spherical precipitates, resulting from the heat treatment. These precipitates were evenly dispersed within the matrix and were identified as the γ' phase. High-magnification SEM was used to measure and calculate an average diameter (which was 67.12 nm for the γ' phase) using ImageJ's particle analysis function.

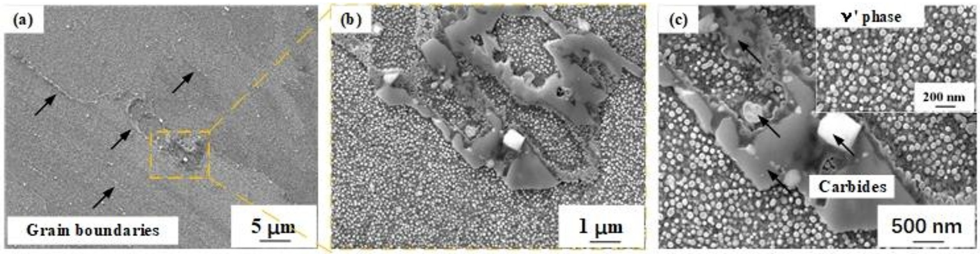

Fig. 3. Secondary electron (SE) imaging SEM micrographs of heat-treated specimens: (a) overview; (b) micrograph near grain boundaries; (c) micrograph in carbides.

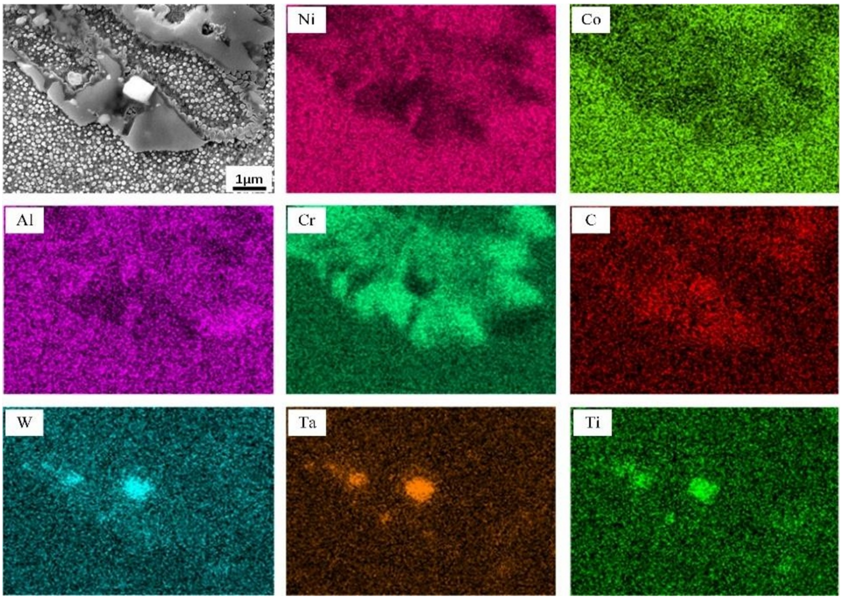

Fig. 4. Energy-dispersive X-ray spectroscopy (EDS) mapping of the precipitates on the grain boundaries in heat-treated specimens.

An energy-dispersive x-ray spectroscopy (EDS) mapping analysis was conducted on the irregular precipitates located at the grain boundaries; the results are shown in Fig. 4. The findings indicate a concentration of Cr, W, Ta, Ti and C in the precipitate regions, while Ni, Co and Al showed depletion. This finding suggests the formation of MC and M23C6 carbide phases [10] at the grain boundaries following heat treatment. Notably, the co-localisation of Cr and C in the darker precipitate areas confirmed the presence of the M23C6 phase. Conversely, the aggregation of W, Ta, Ti and C in the brighter precipitate sites signified the occurrence of the MC phase. During the aging treatment, the MC phase underwent degradation and transformed into both M23C6 and γ' phases, concomitant with γ phase evolution.

3.3 Tensile properties

The tensile testing results of the as-built (AB) LPBF IN738, LTi738 and IN738G specimens are shown in Fig. 5(a). The relatively low elongation (EL, 6.99%) of LPBF IN738 may be attributed to cracking existing in the samples. In contrast, the LTi738 and IN738G samples showed a vastly improved EL (up to 29.92% and 34.76%), due to the absence of hot cracking. The UTS showed a decreasing trend, however, due to the decrease of precipitation strengthening element Ti and grain boundary strengthening element C [7].

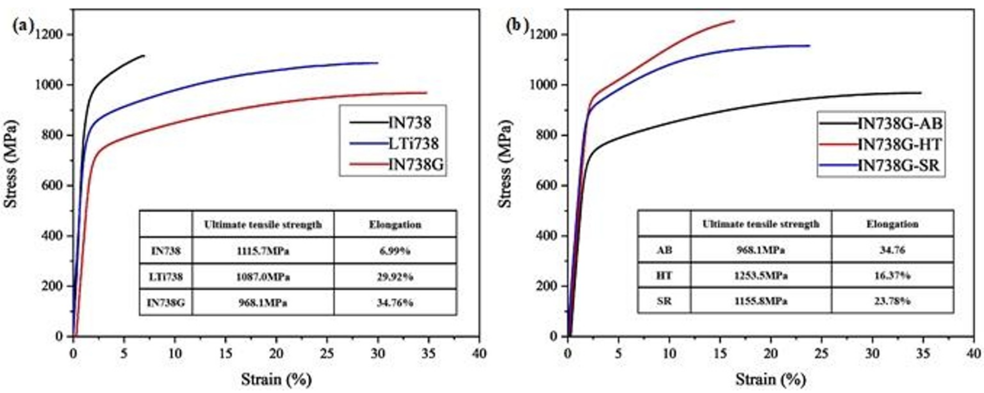

Fig. 5. (a) Tensile testing curves of as-built IN738, LTi738 and IN738G via LPBF; (b) tensile testing curves of LPBF IN738G after heat treatment.

As shown in Fig. 5(b), the UTS of IN738G alloy after stress relief annealing only was 1155.8 MPa, with an EL of 23.78%. The performance was further improved after complete HT; the UTS reached 1253.5 MPa, and the EL was still 16.37%. Therefore, IN738G alloy can realise LPBF forming under normal heat treatment processes and shows good comprehensive mechanical properties.

4 Conclusions

The study's main findings may be summarised as follows:

(1) Different types of defects were observed in LPBF-fabricated IN738, including lack of fusion defects, cracking defects and keyhole defects. The lack of fusion and keyhole defects could be eliminated with appropriate process parameters; the LTi738 and IN738G alloys enabled crack-free LPBF preparation over a wide range of processes.

(2) Heat-treated specimens exhibited continuous carbides along the grain boundaries. EDS mapping revealed enriched Ta, W, Cr, Ti and C, indicative of MC and M23C6 carbides. Uniformly spherical γ' precipitates, averaging 67.12 nm in diameter, were also found within the matrix following heat treatment.

(3) Crack-free LTi738 and IN738G displayed notably superior mechanical properties at room temperature compared to IN738. Both alloys showed substantial elongations of 29.92%

and 34.76%, respectively. Post-HT, IN738G recorded UTS and EL values of 1253.5 MPa and 16.37%, respectively, attributed to γ’ phase precipitation. These results highlight Co’s significant role in boosting overall mechanical performance.

References

1. M. Perrut, P. Caron, M. Thomas, A. Couret, Compt. Rend. Phys, **19**, 657-671 (2018).
2. L.N. Carter, C. Martin, P.J. Withers, M.M. Attallah, J. Alloy. Compd, **615**, 338–347 (2014)
3. Z. Zhang, Q. Han, Z. Liu, L. Wang, H. Zhang, P. Zhao, G. Zhu, C. Huang, R. Setchi, Compos. Part B Eng., **266**, 111023 (2023)
4. C. Guo, G. Li, S. Li, X. Hu, H. Lu, X. Li, Z. Xu, Y. Chen, Q. Li, J. Lu, Q. Zhu, Nano Mater. Sci, **5**, 53-77 (2023)
5. N. J. Harrison, I. Todd, K. Mumtaz, Acta Mater, **94**, 59–68 (2015)
6. H. Wan, Z. Liu, Q. Han, X. Yi. Aer. Sci. Technol, 33, **09**, 26-42 (2022)
7. W. Zhou, Y. Tian, Q. Tan, S. Qiao, H. Luo, G. Zhu, D. Shu, B. Sun, AM, **58**, 103016 (2022)
8. M.M. Attallah, R. Jennings, X. Wang, L.N. Carter, MRS Bull, **41**, 758-764 (2016)
9. J.A. Muñiz-Lerma, Y. Tian, X. Wang, R. Gauvin, M. Brochu, Prog. Addit. Manuf, **4**, 97-107 (2019)
10. H. Zhang, Q. Han, Z. Liu, Z. Zhang, Z. Sui, L. Wang, *Microstructure and Mechanical Properties of IN738C Superalloy Fabricated by Laser Powder Bed Fusion*, in Proceedings of the 10th international Conference on Sustainable Design and Manufacturing, SDM 2023, 18-20 September, 2023, Springer, Singapore (2024)